RSC Advances

PAPER

View Article Online
View Journal | View Issue

Open Access Article. Published on 19 February 2025. Downloaded on 11/10/2025 1:52:29 AM.
This article is licensed under a Creative Commons Attribution-NonCommercial 3.0 Unported Licence.

Check for updates

Cite this: *RSC Adv.*, 2025, **15**, 5665

Luliconazole–niacinamide lipid nanocarrier laden gel for enhanced treatment of vaginal candidiasis: *in vitro, ex vivo, in silico* and preclinical insights

Bhabani Sankar Satapathy,*[a] Ameeduzzafar Zafar,*[b] Musarrat Husain Warsi,[c] Sritam Behera,[d] Dibya Iochan Mohanty,[e] Md Ali Mujtaba,[fg] Mahaprasad Mohanty,[h] Atul Kumar Upadhyay[i] and Mohammad Khalid[j]

A lipid-based nanocarrier system is a novel technique for the delivery of poorly soluble drugs through topical delivery. This study developed a dual-drug (luliconazole: LZ, and niacinamide: NM) loaded lipid nanocarrier (LN)-laden gel for the treatment of vaginal candidiasis. The LNs were prepared using cholesterol and soya-α-lecithin through a thin-film hydration technique. The average vesicle size, polydispersity index, and zeta potential of the optimized LZNMLNs were 126.40 ± 1.30 nm, 0.276, and −34.6 ± 0.8 mV, respectively, and the formulation showed the sustained release of both drugs over an extended period. Selected LZNMLNs were incorporated into a bio-adhesive gel. The optimized LZNMLNs-gel showed excellent viscosity, spreadability, and bio-adhesiveness. The optimized LZNMLNs-gel exhibited significantly higher permeation of LZ (1.46-fold) and NM (1.55-fold) than LZNM gel. The optimized LZNMLNs-gel showed significantly higher *in vitro* antifungal activity (ZOI = 34 ± 2 mm) than commercial Candid V gel (18 ± 1 mm). The optimized LZNMLNs-gel did not show any cytotoxicity against vaginal epithelial cells. The bioavailability of LZNMLNs-gel was significantly ($P < 0.05$) increased (1.94-fold for LZ and 1.33-fold for NM) compared to Candid V, with a decrease in total clearance indicating sustained release of the drug, which may lead to the maintenance of therapeutic concentration for an extended period. *In vivo* antifungal activity showed that the optimized LZNMLNs-gel completely treated the infection on the 7th day of treatment in an induced rabbit model, compared to the commercial gel (Candid V gel, 10 days). Based the findings, it can be concluded that LN-laden gel is an alternative carrier for improvement of the topical delivery of drugs for the treatment of vaginal candidiasis.

Received 27th November 2024
Accepted 11th February 2025

DOI: 10.1039/d4ra08397k

rsc.li/rsc-advances

Introduction

Vaginal candidiasis is a worrying medical challenge as it cannot be treated by conventional therapy.[1] This infection is very invasive and can lead to serious systemic complications unless treated at an early stage. Superficial *Candida* infections subsequently lead to invasive candidiasis, which is very challenging to treat and particularly life-threatening in immune-compromised patients.[2] Around 70% of women globally currently suffer from vulvovaginal candidiasis.[3] Until now, the treatment of vulvovaginal infections has typically involved the use of antifungal drugs in conventional dosage forms, *i.e.*, creams, suppositories, and tablets. However, traditional treatment approaches have some limitations, *i.e.*, sub-therapeutic effectiveness and low patient compliance.[4] Further, localized topical formulations suffer from several limitations, such as a rapid vaginal washout, low absorption, and low bioavailability, with undesirable adverse effects across the vaginal area.[5]

In view of this, nanotechnology-based bio-adhesive gel (nanogel) topical formulation is an effective novel strategy to improve the topical vaginal delivery of therapeutic agents.[6] Bio-adhesive gel laden with lipoidal nanocarriers (LNs, liposomes) is being heavily explored to improve the topical delivery of therapeutic agents for the treatment of topical microbial (fungal or bacterial) infections.[7] LNs are nanosized lipoidal vesicles

[a]GITAM School of Pharmacy, GITAM Deemed to be University, Hyderabad Campus, Telangana-502329, India
[b]Department of Pharmaceutics, College of Pharmacy, Jouf University, Sakaka 72341, Al-Jouf, Saudi Arabia. E-mail: zzafarpharmacian@gmail.com
[c]Department of Pharmaceutics and Industrial Pharmacy, College of Pharmacy, Taif University, Taif 21944, Saudi Arabia
[d]Nityananda College of Pharmacy, Biju Patnaik University of Technology, Sergarh, Balasore, Odisha, India
[e]Centre for Nanomedicine, Department of Pharmaceutics, School of Pharmacy, Anurag University, Hyderabad, Telangana, Pin 500088, India
[f]Department of Pharmaceutics, Faculty of Pharmacy, Northern Border University, Arar, Saudi Arabia
[g]Center for Health Research, Northern Border University, Arar, Saudi Arabia
[h]School of Pharmaceutical Sciences, Siksha 'O' Anusandhan University, Odisha, India
[i]Department of Biotechnology, Thapar Institute of Engineering and Technology, Patiala, Punjab, India
[j]Department of Pharmacognosy, College of Pharmacy, Prince Sattam Bin Abdulaziz University, Al-Kharj 11942, Saudi Arabia

© 2025 The Author(s). Published by the Royal Society of Chemistry

Open Access Article. Published on 19 February 2025. Downloaded on 11/10/2025 1:52:29 AM.
This article is licensed under a Creative Commons Attribution-NonCommercial 3.0 Unported Licence.

composed of biocompatible, non-toxic phospholipid and cholesterol outer layers enclosing an aqueous compartment. Owing to their nano-size and unique hydrophilic and lipophilic properties, LNs have emerged as a promising modality for the delivery of drugs into the body.[8,9] LNs can protect drugs from harsh vaginal environments, target them precisely at the desired site in a controlled manner, and can also modulate their pharmacokinetic (PK) profile.[10] Conversely, bio-adhesive gel possesses the ability to adhere across the vaginal epithelium for an extended period and can prolong the residence time of the drug at the infected area.[11–13]

Luliconazole (LZ), a synthetic imidazole (azole), has been widely used to combat severe fungal infections.[14] It is a broad-spectrum antifungal agent, which selectively inhibits the cytochrome P 450 14-α-demethylase enzyme. It interrupts the alteration of lanosterol to ergosterol and hampers the formation of the fungus cell wall. LZ is poorly water-soluble, which limits its dermal delivery.[15] LZ has been useful for treating superficial fungal infections, genital candidiasis, and chronic mucocutaneous candidiasis. However, following oral administration, there is considerable variation in the LZ absorption concentration and peak plasma concentration. Topical application of the drug through semisolid dosage forms also results in limited systemic availability.[16] Thus, the delivery of LZ through a nanocarrier-based topical formulation could be the preferred strategy to boost its topical delivery and therapeutic effectiveness.

Niacinamide (NM), a vitamin B3 amide, is a well-known dietary supplement with a wide range of therapeutic applications. Currently, it is being widely investigated as a potential therapeutic agent to treat skin diseases. It has various therapeutic, antioxidant, anti-inflammatory, and immunomodulatory properties.[17] Recent studies have documented that NM actively protects skin cells from oxidative stress.[18] Topical delivery of NM improved tissue regeneration in an excisional full-thickness skin wound.[19] Clinical evidence of NM also controls skin aging and pigmentation of skin.[20,21] Thus, delivery of NM along with LZ in a suitable dosage form would improve tissue regeneration and promote the recovery of inflamed tissue in vaginal infection. Hence, co-delivery of LZ- and NM-loaded nanogels would show superior therapeutic efficacy compared to conventional dosage forms. The drug-loaded nanogel would thus maintain higher localized drug availability and would prompt the healing of inflamed tissue while reducing undesirable side effects.

The present study was aimed at developing an LZ- and NM-loaded lipoidal nanocarrier-laden bio-adhesive gel (LZNMLNsG) to treat vaginal candidiasis. The LZLNMLN formulation was developed using the thin-film hydration technique. The LZLNMLNs were evaluated for vesicle characteristics, drug loading and entrapment efficiency. The optimized LZNMLN formulation was incorporated in Carbopol 934P, HPMC-E15M, and neem-gum-based gel systems. The LZLNMLN gel was evaluated for various gel characteristics, *in vitro* release, *ex vivo* permeation, *in vitro* antifungal activity, and cytotoxicity study. A further *in vivo* (pharmacokinetic and pharmacodynamics) study was performed in a rabbit model. An *in silico* docking study was performed to analyze the possible molecular mechanism of LZNMLNs-gel in vaginal candidiasis.

Material and experimental

Materials

LZ and NM were purchased from HiMedia (Maharashtra, India). HPMC E15M was purchased from Dow Chemical Ltd, USA. Soya-α-lecithin (SL) and cholesterol (CHL) were procured from SRL Pvt. Ltd (Maharashtra, India). Butylated hydroxyl toluene (BHT), ascorbic acid, propylene glycol (PG), Sabouraud dextrose agar, 3-(4,5-dimethylthiazol-2-yl)-2,5-diphenyl-2*H*-tetrazolium bromide (MTT), Dulbecco's Modified Eagle's Medium, and fetal bovine serum were procured from HiMedia (Hyderabad, India).

Microorganism. *Candida albicans* were acquired from India's Microbial Type Culture Collection and Gene Bank (MTCC854) in Chandigarh.

Cell line. Primary Vaginal Epithelial Cells (ATCC PCS-480-010) were collected from American Type Culture Collection, Manassas, VA.

Animals. The animal experiment protocol (IAEC/SPS/SOA/127/2023) was approved by the Institute Animal Ethical Committee of Siksha 'O' Anusandhan University, Bhubaneswar, India. The study was performed on female (10–12 weeks, 3.0 ± 0.2 kg) albino rabbits, as per CPCSEA guidelines. All rabbits were acclimated for at least 15 days in a laboratory setting with a regular day and night cycle before the experiment at 25 °C ± 2 °C and 45–55% RH. Nutritious food was given to each rabbit and there was unrestricted access to drinking water throughout the study.

Development of experimental lipid nanocarriers

TLZNMLNs were prepared as per the composition given in Table 1 by using the thin-film hydration method.[22,23] Measured amounts of SL, CHL, and LZ were dissolved in 10 mL of chloroform and transferred to a 250 mL round-bottom flask (RBF). BHT (2% w/v) was added to the solution to prevent lipid peroxidation. RBF was placed in a rotary evaporator (Rotavap, Heidolph, Germany) to evaporate the chloroform. The resultant thin lipid film was formed and stored overnight in a desiccator. Hydration of the dried lipid film was undertaken using a phosphate buffer solution (pH 7.4) containing a measured amount of NM. Then the dispersion was subjected to ultrasonication (digital ultrasonic cleaner, Mumbai, India) for 30 min (30 s intervals) for the formation of unilamellar nanosize vesicles. The resultant formulation was kept for 1–2 h at 25 °C to allow the discrete nano-vesicles to regain their native form. Then the vesicle dispersion was subjected to centrifugation at 16 000 rpm (45 min at 4 °C). The resultant sediment was collected in a Petri dish and stored at −4 °C followed by lyophilization for 8–10 h (laboratory freeze dryer, Mumbai, India) to obtain freeze-dried LZNMLNs.

Vesicle characterization

The average vesicle size (Z-avg), polydispersity index (PDI), and zeta potential of the LZNMLNs were determined with a zeta

 © 2025 The Author(s). Published by the Royal Society of Chemistry

Open Access Article. Published on 19 February 2025. Downloaded on 11/10/2025 1:52:29 AM.
This article is licensed under a Creative Commons Attribution-NonCommercial 3.0 Unported Licence.

Table 1 Formulation composition, % drug loading and entrapment efficiency % of luliconazole- and niacinamide-loaded lipid nanocarriers[a]

Formulation code	Ratio of CHL and SL	Amount of drug (mg)		% Drug loading		EE	
		LZ	NM	LZ	NM	LZ	NM
LZNMLNs-1	1 : 1	10	10	5.38 ± 0.40	3.96 ± 0.20	59.9 ± 0.50	51.3 ± 1.41
LZNMLNs-2	1 : 2	10	10	10.35 ± 0.60	9.13 ± 0.70	72.1 ± 1.71	70.1 ± 0.70
LZNMLNs-3	1 : 1.5	10	10	7.89 ± 0.30	7.95 ± 0.40	63.2 ± 0.70	67.2 ± 0.21

[a] LZ, luliconazole; NM, niacinamide; LZNMLN, luliconazole- and niacinamide-loaded lipid nanocarriers; SL, soya-L-α-lecithin; CHL, cholesterol; EE, entrapment efficiency. Data show mean ± SD ($n = 3$).

sizer (Nano ZS 90, Malvern Instruments Ltd, UK). The lyophilized LZNMLN formulation was diluted with deionized water followed by sonication for 5–7 min to make agglomerate-free nano-vesicles. The sample was then placed into a cuvette and analyzed at 25 ± 0.5 °C using the dynamic light scattering method.[23,24]

Entrapment efficiency (EE) and drug loading

The lyophilized LZNMLN (5 mg) formulation was dispersed in a mixture of acetonitrile and ethanol (1 : 1 v/v). The nano-dispersion was sonicated and centrifuged at 16 000 rpm for 5 min. The dispersion was filtered, and the concentration of LZ and NM was analyzed with a UV spectrophotometer (Shimadzu 1800, USA) at 296 nm and 260 nm. The % drug loading and EE were calculated as follows:

$$\%\text{EE} = \frac{\text{Theoretical drug conc} - \text{drug conc in supernatant}}{\text{Theoretical drug conc}} \times 100$$

$$\%\text{Drug loading} = \frac{\text{Theoretical drug conc} - \text{drug conc in supernatant}}{\text{weight of LZNMLNs}} \times 100$$

Fourier-transform infrared spectroscopy (FTIR)

This study identified possible drug–excipient interactions by analyzing the primary wavenumbers of the functional groups.[25] The spectra of pure LZ, NM, SL, CHL, BHT, physical mixtures, and optimized LZNMLNs were analyzed using an FTIR spectrophotometer (Shimadzu IR Prestige-21, Mumbai, India). The samples were scanned between 4000 and 500 cm^{-1} at 25 °C. The spectra were recorded and compared with each other.

Differential scanning calorimetry (DSC)

A DSC instrument (Mettler Toledo DSC-1, Switzerland) was used to measure the change in enthalpy in the samples with respect to temperature.[23,25] Weighed amounts of pure LZ, NM, and optimized LZNMLNs were separately packed into an aluminum pan and placed inside a DSC chamber under a dynamic nitrogen environment (50 mL min^{-1}). The sample was scanned between 30 and 200 °C at a rate of 10 °C min^{-1}.

X-ray diffraction analysis (XRD)

An X-ray diffractometer (D8 Discover, Bruker, Germany) was employed to study the XRD analysis of the sample to explain the crystallinity/amorphous nature of the sample.[26] The LZ, NM, and optimized LZNMLNs were separately used to fill the sample holder, making the thin layer. The sample was scanned between 5 and 70° at the 2-theta level (1° min^{-1} scanning speed).

Field emission scanning electron microscopy (FESEM)

FESEM is a powerful method for the high-resolution surface imaging of lipoidal nanocarriers.[27,28] Briefly, lyophilized optimized LZNMLNs were spread over a piece of carbon tape across a stub and vacuum-dried, followed by the application of a platinum coating over the surface to improve the resolution, and analyzed with a scanning electron microscope (FESEM, Carl Zeiss Microscopy GmbH, Jena, Germany).

Cryo-transmission electron microscopy (cryo-TEM)

The optimized LZNMLNs were dispersed in deionized water, sonicated (5 min), and immediately vitrified over a cryo-stage inside liquid ethane. About 4 μL of sample suspension was applied over a clean grid and preserved under liquid nitrogen. The sample was analyzed using an FEI Tecnai G2 X-Twin Cryo-TEM microscope (FEI, Hillsboro, OR, USA) at 200 kV accelerated voltage.[29]

In vitro drug release and release kinetics

The dialysis method was used to analyze the release of LZ and NM from the LZNMLNs. In brief, a measured 10 mg of LZNMLNs (containing 1.03 mg of LZ and 0.79 mg of NM) was placed in a dialysis bag (MWCO: 3.5 kDa) and submerged in 50 mL of phosphate buffer saline (PBS, pH 7.2).[30] The release medium was stirred at 100 rpm and maintained at 37 °C throughout the experiment. Aliquots of 1 mL of release medium were taken at pre-fixed time intervals, and the same volume of

Open Access Article. Published on 19 February 2025. Downloaded on 11/10/2025 1:52:29 AM.
This article is licensed under a Creative Commons Attribution-NonCommercial 3.0 Unported Licence.

PBS was added to the beaker to maintain a constant volume. The concentration was analyzed using a UV-visible spectrophotometer at 296 nm for LZ and 260 nm for NM against PBS as a blank. The drug release data of the LZNMLNs was plotted against time according to different models, *viz.*, zero-order, first-order, Higuchi, and Korsmeyer–Peppas, and R^2 values were calculated for each model for identification of the best-fitting model.[31]

Preparation of LZNMLN-loaded gel

LZNMLN-loaded gel was prepared using Carbopol 934P, HPMC E15M and *Azadirachta indica* gum polymers as per the composition given in Table 2. Different concentrations of Carbopol 934P were dispersed under constant magnetic stirring (300 rpm). Then the required quantity of HPMC-E15M was mixed into the Carbopol 934P and stirred overnight. Then *Azadirachta indica* gum was dispersed in mildly heated distilled water. Then it was mixed with the Carbopol934P/HPMC HPMC-E15M dispersion under continuous stirring. Ascorbic acid and propylene glycol (PG) were added to the dispersion system. The required amount of LZNMLNs (1% w/w) was dispersed using 0.1% Span 80 and added to the aqueous polymeric dispersion system while stirring continuously. Finally, the pH of LZNMLN-loaded gel was adjusted using 10% w/v NaOH solution.

Characterization of LZNMLNs-gel

Homogeneity and smoothness. To determine their homogeneity, the LZNMLNs-gels were visually inspected for the presence of any insoluble particulate matter. The smoothness or grittiness of the LZNMLNs-gels was analyzed by rubbing them between the fingers.

pH. A pH meter (NEL Mod.821, Turkey) was used to measure the pH of the LZNMLNs-gels. The LZNMLNs-gels (1 g) were separately dispersed in 100 mL of deionized water at 25 °C.[32] The electrode was dipped for 2 min, and the pH was recorded in triplicate.

Viscosity. The viscosity of the LZNMLNs-gels was measured using a Brookfield viscometer (DV III Ultra V6.0, Brookfield Engineering Laboratories, Inc., Middleboro, MA).[33]

Spreadability. The spreadability of the LZNMLNs-gels was determined according to their conventional slip and drag properties, as described by Sudipta *et al.*[34] Briefly, a measured amount of LZNMLNs-gel was sandwiched between two slides, with excess amounts of gel scraped off. The upper slide was attached to a given weight of 80 g through a string (passed over a pulley), which was then allowed to pull over the lower slide. The time (in seconds) during which the slides were detached from each other was recorded, and the spreadability was calculated with the reported formula.[35] In general, the shorter the time of separation, the better the spreadability.

Extrudability. The LZNMLNs-gels were packed into a foldable aluminum tube with a standard cap. After that, the tubes were sandwiched between two glass slides and clamped. The covers were removed and a 200 g weight was added over the slides. The extruded volume of each LZNMLNs-gel was taken and weighed. The % percentage extrudability of the gels was determined:[34]

$$\text{Extrudability} = \frac{\text{extrudability amount}}{\text{weight of gel}} \times 100$$

Swelling. LZNMLNs-gels were deposited into 20 mL of PBS (pH 4.2) at 25 °C. At pre-scheduled intervals, *i.e.* 2, 4, 6, and 8 h, the gels were weighed and the % swelling was calculated:[36]

$$\%\text{Swelling} = \frac{\text{weight at definite time} - \text{initial weight}}{\text{initial weight}} \times 100$$

Bio-adhesion. The usual arm balancing method was used to evaluate the adhesion behavior of the LZNMLNs-gels.[37] A container with a balancing load on one side and a balance with two glass plates on the other comprised the tool. The base of the stage held the lower of the two glass plates, while a chain connected the upper plate to the balancing arm. The mucosal membrane of a goat, following proper cleaning and perfusing with saline, was trimmed to the appropriate size. The mucosal side was exposed to the gel side by applying adhesive to two portions of the membrane that were attached between two glass plates. After placing the measured amount of LZNMLNs-gels (100 mg), the upper glass plate was subjected to a 10 min pre-loaded squeeze (35 g). Following the removal of the pre-load, the glass plates were separated from each other under the trickling of water from a specific height. The weight of water needed for the detachment of the glass slides was correlated with the bio-adhesion force.

Rheological properties. Rheological studies of the optimized LZNMLNs-gel and commercial gel (Candid V) were carried out with a moving-die rheometer (Ektron Tek Co. Ltd, Taiwan) at 37 °C. At shear rates ranging from 1 to 60 per sec, the viscosity of

Table 2 Formulation composition of luliconazole- and niacinamide-loaded lipid nanocarrier incorporated bio-adhesive gels

Composition	LZNMLNs2G1	LZNMLNs2G2	LZNMLNs2G3
Carbopol 934P (%w/w)	1	0.8	0.5
HPMC E15M (%w/w)	0.5	1.5	1
Azadirachta indica gum (% w/w)	1	0.5	1.5
Propylene glycol	5 mL	5 mL	5 mL
Ascorbic acid	4 mg	4 mg	4 mg
LZNMLNs2	30 mg	30 mg	30 mg
Span 80 (%)	0.5	0.5	0.5
10% NaOH solution	q.s	q.s	q.s
Double distilled water	50 mL (q.s.)	50 mL (q.s.)	50 mL (q.s.)

 © 2025 The Author(s). Published by the Royal Society of Chemistry

Open Access Article. Published on 19 February 2025. Downloaded on 11/10/2025 1:52:29 AM. This article is licensed under a Creative Commons Attribution-NonCommercial 3.0 Unported Licence.

both gels was analyzed, and a graph between viscosity and shear rate was plotted.[38]

***Ex vivo* drug permeation.** An excised goat vaginal mucosal membrane was used for the analysis of the *ex vivo* permeation of LZ and NM from optimized LZNMLNs-gel. The membrane was mounted between Keshary–Chien diffusion cells (20 mL with 1.766 cm^2 cross-sectional area).[39] The receptor part of the diffusion cell was filled with PBS (pH 4.2, simulated vaginal fluid) and maintained at 37 °C and stirred at 50 rpm. The donor part of the diffusion cell was filled with optimized LZNMLNs-gel (1%). At pre-determined intervals, 1 mL aliquots were taken from the receptor compartment and simultaneously replaced with fresh PBS. The permeation concentration of LZ and NM was analyzed with a UV-spectrophotometer at 296 nm for LZ and 260 nm for NM. The flux and apparent permeability coefficient were calculated.

***In vitro* antifungal activity.** The *in vitro* antimicrobial effectiveness of the optimized LZNMLNs-gel against *Candida albicans* (1.5×10^8 CFU mL^{-1}) was evaluated by the agar well diffusion method.[40] Briefly, Sabouraud dextrose agar (SDA) medium was prepared and sterilized at 121 °C for 15 min. The *Candida albicans* (MTCC854) and melted SDA medium were poured into a sterilized Petri plate and allowed to solidify. A 6 mm hole was made using a sterile borer. Measured amounts of LZNMLNs-gel (containing 1% w/v of LZ and NM) and commercial gel (Candid V gel, 1%) were incorporated into the agar hole. The plate was incubated at 25 °C for 48 h and the zone of inhibition (ZOI) was measured.

Cytotoxicity evaluation in vaginal cell line. An MTT assay was used to determine the cell viability of primary vaginal epithelial cells (ATCC PCS-480-010) treated with optimized LZNMLNs gel.[41] Briefly, the vaginal epithelial cells (at 1×10^4 cells) were grown in Dulbecco's Modified Eagle Medium (DMEM) supplemented with 10% fetal bovine serum and incubated in a CO_2 incubator for 24 h (37 °C). L-Glutamine, and penicillin–streptomycin (1%) were added into the medium. The cells were plated into 96-well microplates and different concentrations of optimized LZNMLNs-gel, *i.e.*, 200, 400, 600, 800, 1000, and 1200 μg mL^{-1} were added. The plates were incubated for 48 h. 100 μL of 3-(4,5-dimethylthiazol-2-yl)-2,5-diphenyltetrazolium bromide (MTT) was added into each micro-plate well and again incubated for 4 h. Following the removal of the culture medium, sterile dimethyl sulfoxide (100 μL) was added into each culture well, resulting in the solubilization of formazan crystals. The absorbance of the sample was measured at 570 nm using a microplate reader (Multiskan™ FC microplate photometer, Thermo Scientific, India) and the % viability was calculated.[42]

Pharmacokinetic study. A pharmacokinetic study of optimized LZNMLNs-gel was conducted on laboratory white albino rabbits (female, 3.0 ± 0.2 kg) and was compared with that of Candid V gel. The rabbits were divided into two experimental groups: Group I for optimized LZNMLNs-gel, and Group II for Candid V gel. The rabbits were kept fasting overnight before the study. Blood samples were taken before application of the formulation for baseline correction. The optimized LZNMLNs-gel and Candid V gel (1% w/w) were applied to the vaginal area of the rabbits. At different time intervals, the rabbits were anesthetized using a diethyl ether inhaler. The blood samples were collected into EDTA tubes. The plasma was separated by centrifugation of the blood at 5000 rpm (10 min) using a microcentrifuge (Inovia Technology, INO-FBC 5000, Germany). For extraction of LZ and NM, 100 μL of each plasma sample was mixed with acetonitrile : ethanol (1 mL, 1 : 1). Then the mixture was centrifuged at 5000 rpm for 15 min, and the supernatant was collected. Then the supernatants were dried under a vacuum dryer. The dried samples were reconstituted with a mobile phase (acetonitrile : methanol) and 50 μL of carbamazepine solution (internal standard). For the analysis, 20 μL of the sample was injected into the LCMS/MS column (Discovery C18, 15 cm × 2.1 mm ID, 5 μM). Using Phoenix WinNonlin software, various pharmacokinetic parameters *i.e.*, C_{max}, T_{max}, the area under the curve (AUC), half-life ($t_{1/2}$), mean time of residence (MRT), the area under the first moment curve (AUMC), and elimination rate (K_{el}), were determined.[43]

***In vivo* efficacy evaluation in rabbit vaginitis model.** Animal experiments were conducted according to the CCSEA Animal Guidelines for Ethical Review of Animal Welfare. The study was done on female albino rabbits. The rabbits were divided into three treatment groups: Group I (optimized LZNMLNs-gel), Group II (Candid V gel), and Group III (blank gel). The rabbits received an estradiol valerate injection (1.2 mg kg^{-1}) to develop the required immunosuppressive environment and false estrus prior to infection. To induce infection, about 100 μL of *Candida albicans* cell suspension (3×10^8 CFU per mL with FBS (10%)) was inoculated into a rabbit vagina using an automatic micropipette, once a day for five consecutive days.[44] To stop fluid from leaking out, the vaginal orifice was closed with aseptic cotton balls. After five days of inoculation, the vulval redness, swelling, secretions, *etc.* were recorded. The formulation, *i.e.*, optimized LZNMLNs-gel (1 g of gel was equivalent to 1.03 mg of LZ and 0.79 mg of NM), Candid V gel, and blank gel were applied to the respective group for 10 days. The observation was done visually.

Docking analysis. To predict the interaction proficiency of drugs with selected *Candida* proteins, an *in silico* docking study was conducted. Two-dimensional structures of LZ and NM were obtained *via* the PubChem website.[45] The Protein Data Bank provided the target protein crystal structures.[46] The dehydration of all proteins, ligand separation, and storage with molecular docking was conducted using AutoDockTools1.5.6.25. The docking outcome was modified for the optimal structure and visualized with Discovery Studio Visualizer 2.5. From the docking score, the protein–ligand interaction proficiency was predicted.

Statistical analysis. Average ± standard deviation (SD) was used to express the data. A one-way analysis of variance (ANOVA) and a Tukey *post hoc* test were applied for statistical analysis (OriginPro 8, MA USA). $P < 0.05$ was considered at the 95% confidence level for significant differences.

Results

Vesicle characterization

The average vesicle size (Z-avg) of the LZNMLN formulations was analyzed and found to be 184.60 ± 5.01 nm for LZNMLNs1,

Open Access Article. Published on 19 February 2025. Downloaded on 11/10/2025 1:52:29 AM.
This article is licensed under a Creative Commons Attribution-NonCommercial 3.0 Unported Licence.

126.40 ± 1.30 nm for LZNMLNs2, and 211.3 ± 8.1 nm for LZNMLNs3. The PDI of the formulations was found to be 0.801 for LZNMLNs1, 0.376 for LZNMLNs2, and 0.621 for LZNMLNs3. The zeta potential of the formulations was found to be −39.61 mV for LZNMLNs1, −34.6 mV for LZNMLNs2, and −26.16 mV for LZNMLNs3. The vesicle size and PDI of LZNMLNs2 were found to be lower (PDI < 0.5) than for the other formulations (LZNMLNs1 and LZNMLNs3).

Drug loading and entrapment efficiency

The drug loading and EE of LZ and NM in the LZNMLNs were analyzed, and the results are depicted in Table 1. The loading of LZ ranged from 5.38% (LZNMLNs1) to 10.35% (LZNMLNs2). However, the loading of NM ranged from 3.96% (LZNMLNs1) to 9.13% (LZNMLNs2). The EE of LZ was found to range from 59.9 ± 0.5% (LZNMLNs1) to 72.1 ± 1.7 (LZNMLNs2). However, the EE of NM ranged from 51.3 ± 14% (LZNMLNs1) to 70.1 ± 0.7% (LZNMLNs2).

Selection of optimized LZNMLNs

The optimized LZNMLN formulation was selected based on optimum parameters value, *i.e.*, Z-avg, drug loading %, and EE. Among the formulations, LZNMLNs2 was selected as the optimized batch, showing Z-avg of 126.40 ± 1.30 nm, PDI of 0.376, and EE of −34.6 mV (Fig. 1A and B). The loadings of LZ and NM in LZNMLNs2 were found to be 10.35%, and 9.13%, respectively, with satisfactory EE as well (Table 1). Based on the characterization data, LZNMLNs2 was used for further study.

FESEM analysis

The surface morphology of the LZNMLNs2 is displayed in Fig. 1C. The shape of LZNMLNs2 displayed a spherical and smooth surface. No agglomeration was found throughout the sample.

Cryo-TEM analysis

The cryo-TEM image of LZNMLNs2 showed a spherical lipid layer with an inner aqueous compartment (Fig. 2D). Furthermore, the outer surface is smooth and spherical without any perforations, confirming its stability.

FTIR-ATR analysis

The FTIR spectra of the LZ, NM, SL, CHL, BHT, physical mixtures, and optimized LZNMLNs are shown in Fig. 2A.

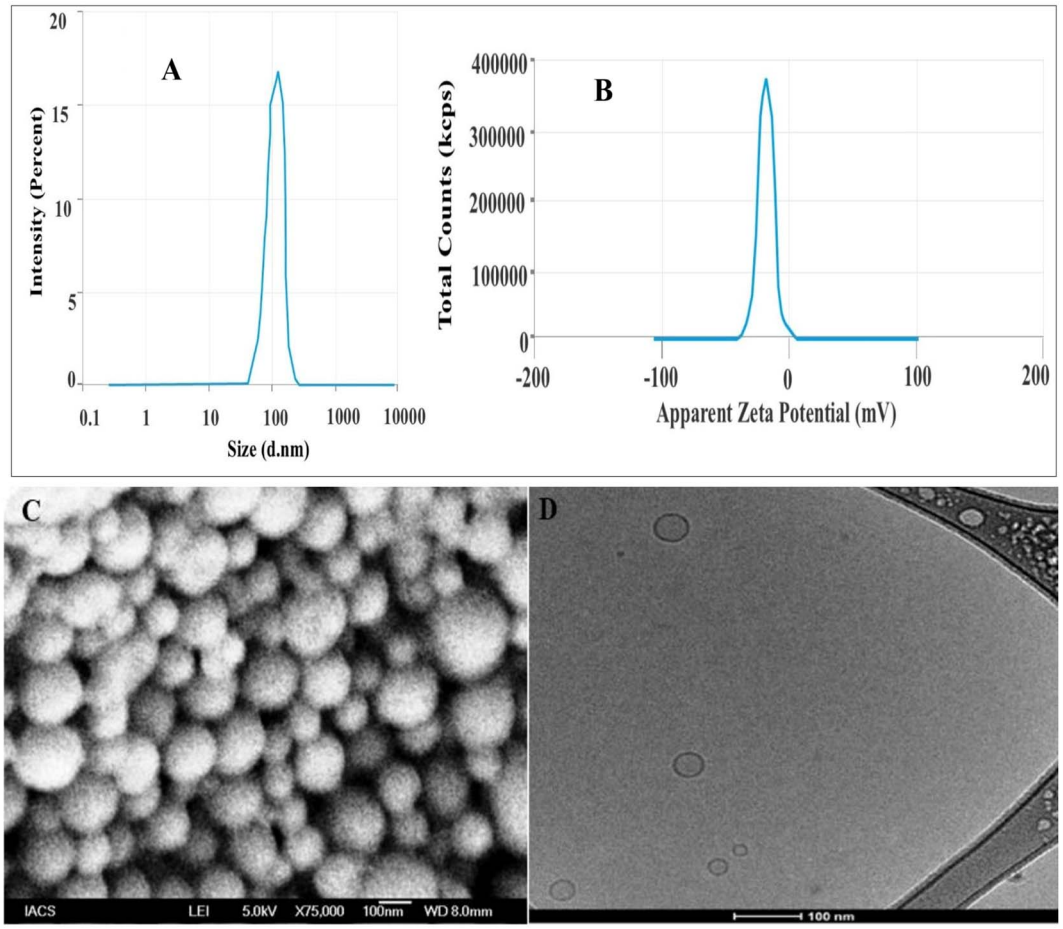

Fig. 1 (A) Average vesicle size (Z-avg), (B) zeta potential, (C) field emission scanning electron microscopy, and (D) cryo-transmission electron microscopy of optimized luliconazole- and niacinamide-loaded lipid nanocarriers (LZNMLNs2).

 © 2025 The Author(s). Published by the Royal Society of Chemistry

Open Access Article. Published on 19 February 2025. Downloaded on 11/10/2025 1:52:29 AM.
This article is licensed under a Creative Commons Attribution-NonCommercial 3.0 Unported Licence.

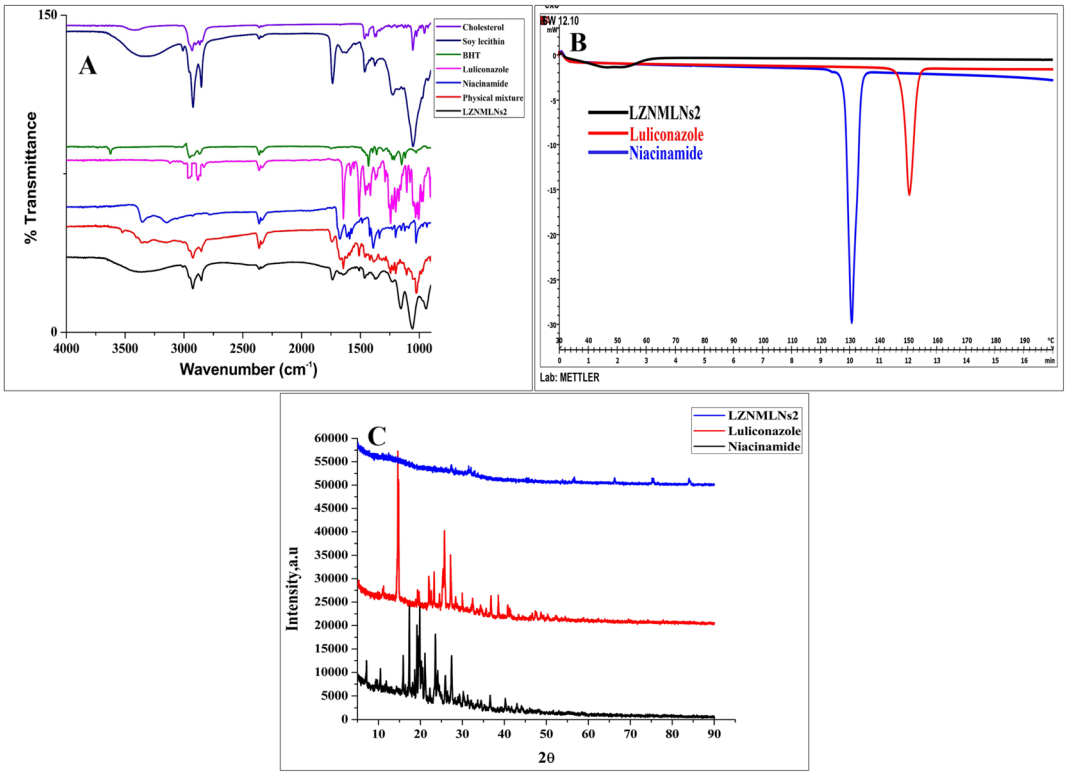

Fig. 2 (A) FTIR study of LZ, NM, SL, CHL, BHT, physical mixture and optimized LZNMLNs. (B) DSC thermogram of LZ, NM and optimized LZNMLNs. (C) XRD diffractograms of LZ, NM and optimized LZNMLNs (LZNMLNs2).

Characteristic peaks of LZ were observed at 905.41 cm^{-1} (C–Cl stretching), 1644.98 cm^{-1} (C=C alkene stretching), 2200 cm^{-1} (CN stretching), and 2830.09 cm^{-1} (C–H aliphatic stretching), confirming its purity. Similarly, the FTIR spectrum of NM showed characteristic peaks at 1672.95 cm^{-1} (C=O stretching), 3353.6 cm^{-1} (N–H stretching), and 1614.13 cm^{-1} (N–H bending), confirming its purity. In the FTIR spectrum of the physical mixture (SL, CHL, BHT, and drugs), characteristic peaks were found at 1742.37 cm^{-1} corresponding to C=O stretching of the ester in SL, 2924.52 cm^{-1} for O–H stretching in CHL, 1644.98 cm^{-1} for C=H stretching in LZ, 3359.39 cm^{-1} for N–H stretching in NM, *etc.* This showed no significant alteration in the characteristic peaks of the drugs or excipients in the physical mixture of ingredients, confirming the absence of incompatibility. The FTIR spectrum of LZNMLNs2 further showed that the characteristic peaks of the drugs at 2852.2 cm^{-1} (C–H aliphatic stretching in LZ) and 1646.91 cm^{-1} (N–H bending or C=O stretching in NM) were retained with only slight shifting, indicating no interaction between drugs and excipients.

DSC analysis

The physiochemical state, such as crystalline behavior or degradation profile, including any chemical interactions in the formulation, was evaluated using DSC. The thermogram showed a clear, sharp, single endothermic peak for pure LZ at 153.3 °C and for NM at 133.84 °C, corresponding to their melting points, which confirms the crystalline nature of the drugs (Fig. 2B). However, in the thermogram of LZNMLNs2, clear sharp peaks were absent, which indicated encapsulation of the drugs inside the lipoidal core/bilayer matrix and loss of crystallinity. Additionally, no additional endothermic peaks appeared in LZNMLNs2, not even in the molten state, which supported the absence of any chemical interactions between drugs and lipid components.

XRD analysis

The XRD diffractogram of pure LZ showed characteristic peaks at 17.38°, 19.82°, 21.08°, 23.5°, and 27.37° with corresponding intensities of 2455 (58), 2202 (54), 1778 (41), 1516 (119), and 2125 (55), respectively. Similarly, NM characteristic peaks were detected at 14.80°, 14.61°, 25.69°, and 27.18° with corresponding intensities of 2759 (358), 2127 (171), 1998 (193), and 1496 (66), respectively (Fig. 2C). These sharp peaks with high intensity confirmed the crystalline nature of both LZ and NM. However, the diffractogram of LZNMLNs2 did not show the sharp and distinct peaks of LZ and NM; rather, diminished peaks with a significant reduction in peak height and area were observed. The overall analysis indicated the amorphisation of LZ and NM into the LZNMLNs2 matrix.

In vitro drug release and release kinetics

The *in vitro* release study of LZ and NM from LZNMLNs2 was done by the dialysis bag method in simulated vaginal fluid (PBS,

Open Access Article. Published on 19 February 2025. Downloaded on 11/10/2025 1:52:29 AM.
This article is licensed under a Creative Commons Attribution-NonCommercial 3.0 Unported Licence.

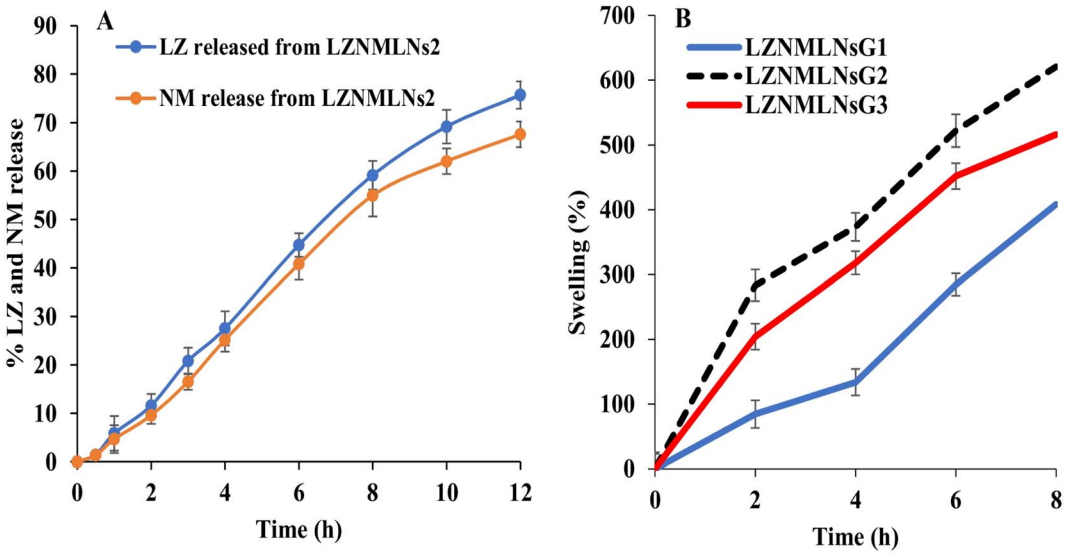

Fig. 3 (A) *In vitro* drug release study of LZ and NM from optimized LZNMLNs2. (B) % Swelling of different LZNMLNsG at different time intervals.

pH 4.2), and the results are shown in Fig. 3A. Both drugs (LZ and NM) were appropriately released from LZNMLNs2 without any burst release. The release of LZ and NM from LZNMLNs2 was 75.71 ± 2.79% and 67.61 ± 2.65%, respectively, in 12 h. The study showed that LZ and NM were released from LZNMLNs2 in a sustained manner without any fluctuation (burst release). This revealed that both drugs were successfully encapsulated into the lipid matrix. The first-order kinetic release model was found to give the best fit (R^2 values of 0.9925 and 0.9921 for LZ and NM), which suggests that the drug release might follow the process of diffusion and erosion from the nano-lipoidal vesicles.

Development and characterization of experimental LZNMLN gel

The optimized LZNMLNs (LZNMLNs2) were successfully incorporated into a gel system using a gelling polymer (Carbopol and HPMC) and evaluated. *Azadirachta indica* gum was used to aid sufficient bio-adhesion. The results of all evaluation parameters are depicted in Table 3. The pH of all LZNMLNs2-loaded gels (LZNMLNs2G) was found to range from 4.32 ± 0.10 to 4.56 ± 0.22, which is very close and compatible with vaginal pH (4.5). The viscosity of the gels was in the range of 34 231 ± 68 cps (LZNMLNs2G1) to 43 126 ± 84 cps (LZNMLNs2G2) (Table 3). The viscosity of the gel increased with an increase in polymer concentration. The spreadability of the gels was found to be 6.82 ± 0.12 g cm per sec for LZNMLNs2G1, 5.03 ± 0.42 g cm per sec for LZNMLNs2G2, and 5.92 ± 0.24 g cm per sec for LZNMLNs2G3 (Table 3). The spreadability of gel depended on viscosity (polymer concentration) of the gel. The extrudability of the gel was analyzed and found to be (91.04 ± 0.17% for LZNMLNs2G1, 78.2 ± 0.78% for LZNMLNs2G2), and 83.43 ± 1.5% for LZNMLNs2G3. The bio-adhesive strength of all developed gels was found to be satisfactory at 19.61 ± 2.31 g for LZNMLNs2G1, 26.32 ± 1.02 g for LZNMLNs2G2, and 21.23 ± 1.14 g for LZNMLNs2G3 (Table 3).

Swelling study

The swelling study of the gels was determined, and the results are depicted in Fig. 3B. LZNMLNs2G2 showed satisfactory swelling, *i.e.*, 620.56 ± 25.29%, compared to LZNMLNs2G1 (408.34 ± 17.19%) and LZNMLNs2G3 (516.32 ± 19.99%) over an 8 h study period.

Selection of optimized LZNMLNs2G

The LZNMLNs2G2 was selected as an optimized formulation based on viscosity, spreadability, extrudability, bio-adhesive strength, and swelling, and thus it was selected for further analysis of *in vitro* and *in vivo* efficacy.

Table 3 Physical characterization of luliconazole- and niacinamide-loaded lipid nanocarrier incorporated adhesive gels

Formulation	pH	Viscosity (cps)	Mucoadhesive strength (gf)	Spreadability (g cm per sec)	Extrudability (%)
LZNNLNs2G1	4.34 ± 0.12	34 231 ± 68	19.61 ± 2.31	6.82 ± 0.12	91.04 ± 0.17[b]
LZNNLNs2G2	4.32 ± 0.10	43 126 ± 84	26.32 ± 1.02	5.03 ± 0.42	78.2 ± 0.78[a]
LZNNLNs2G3	4.56 ± 0.22	39 092 ± 92	21.23 ± 1.14	5.92 ± 0.24	83.43 ± 1.5[b]

[a] Excellent. [b] satisfactory.

 © 2025 The Author(s). Published by the Royal Society of Chemistry

Open Access Article. Published on 19 February 2025. Downloaded on 11/10/2025 1:52:29 AM.
This article is licensed under a Creative Commons Attribution-NonCommercial 3.0 Unported Licence.

Rheological properties

The flow curve of LZNMLNs2G2 and the commercial formulation showed satisfactory rheological characteristics (Fig. 4A). The viscosity of the gel decreases by increasing the shear rate. It exhibited a shear-thinning system, *i.e.*, pseudo-plastic flow (non-Newtonian flow).

Ex vivo permeation study

The *ex vivo* permeation of LZ and NM from LZNMLNs2G2 was studied using the excised goat mucosa, and results are represented graphically in Fig. 4B. The % permeation of LZ and NM from LZNMLNs2G2 was found to be 61.08 ± 3.59% (1832.60 ± 107.61 μg) and 56.74 ± 1.87% (1702.17 ± 56.09 μg), respectively. The % permeation of LZ and NM from plain LZNM-gel was found to be 41.74 ± 2.98% (1252.17 ± 89.35 μg) and 36.52 ± 2.65% (1095.65 ± 79.56 μg), respectively. The flux of LZ and NM from LZNMLNs2G2 was found to be 246.32 ± 14.46 μg cm^{-2} h^{-1} and 228.78 ± 7.54 μg cm^{-2} h^{-1}, respectively. It was observed that LZNMLNs2G2 exhibited a 1.46-fold higher permeation of LZ than plain LZNM gel and a 1.55-fold higher permeation of NM than plain LZNM gel.

In vitro antimicrobial efficacy evaluation against *Candida albicans*

The antimicrobial activity of LZNMLNs2G2 (1 μg mL^{-1} drug concentration) against *Candida albicans* was studied and compared with Candid V gel (clotrimazole, 1% w/w) and control (DMSO) (Fig. 5A). The ZOI of LZNMLNs2G2 and Candid V gel was analyzed and found to be 34 ± 2 mm and 18 ± 1 mm, respectively. In general, antimicrobial potency is classified as sensitive (ZOI ≥ 11 mm), intermediate (ZOI, 8–10 mm), or resistant (ZOI < 7 mm).[47] The area of ZOI around LZNMLNs2G2 was a little hazy compared to the ZOI of Candid V gel, which could be attributed to the slower/sustained release of drugs from the LZNMLNs2G2. This revealed that LZNMLNs2G2 exhibited significantly ($P < 0.05$) higher antimicrobial activity than Candid V gel against *Candida albicans*.[48]

Cytotoxicity study in vaginal epithelial cells

The cytotoxicity of LZNMLNs2G2 and blank gel was evaluated by the MTT assay method on vaginal epithelial cells (ATCC PCS-480-010), and the results are depicted in Fig. 5B. A negligible reduction in the cell viability was observed in vaginal epithelial cells with LZNMLNs2G2, *i.e.*, 91.83 ± 4.91%, 88.78 ± 3.31%, and 86.75 ± 3.29%, was observed at 800 μg mL^{-1}, 1000 μg mL^{-1}, and 1200 μg mL^{-1}, respectively. Thus, the results showed no significant reduction in cell proliferation even after 24 h of incubation at various tested concentrations. The results indicated that LZNMLNs2G2 is non-toxic even at higher concentrations. The blank gel (no drugs) also did not adversely affect vaginal epithelial cells, indicating the biocompatible nature of the excipients used for the preparation of LZNMLNs2G2.

Pharmacokinetic study (PK)

A pharmacokinetic study of the LZNMLNs2G2 and commercial gel (Candid V) was performed on the rabbits and the plasma concentration *vs.* time graph is depicted in Fig. 6A and the PK data is given in Table 4. The PK graph clearly showed higher residence of LZ and NM in plasma delivered through LZNMLN2G2 compared to LZNM gel. The T_{max}, C_{max}, $AUC_{0\text{-}t}$, K_{el}, $AUC_{0\text{-}inf}$, $AUMC_{0\text{-}t}$, $AUMC_{0\text{-}inf}$, half-life and MRT of LZ from LZNMLNs2G2 were found to be 4 h, 927.63 ± 38.667 ng mL^{-1}, 10 110.88 ± 143.87 ng h mL^{-1}, 0.087 ± 0.021 h^{-1}, 11 828.00 ± 103.87 ng h mL^{-1}, 83 542.28 ± 172.18 ng h^2 mL^{-1}, 144 276.01 ± 202.12 ng h^2 mL^{-1}, 7.88 ± 0.21 h, and 8.26 ± 0.24 h, respectively. However, the T_{max}, C_{max}, $AUC_{0\text{-}t}$, K_{el}, $AUC_{0\text{-}inf}$, $AUMC_{0\text{-}t}$, $AUMC_{0\text{-}inf}$, half-life and MRT of NM from LZNMLNs2G2 were found to be 4 h, 769.21 ± 43.67 ng mL^{-1}, 6944.10 ± 78.93 ng h

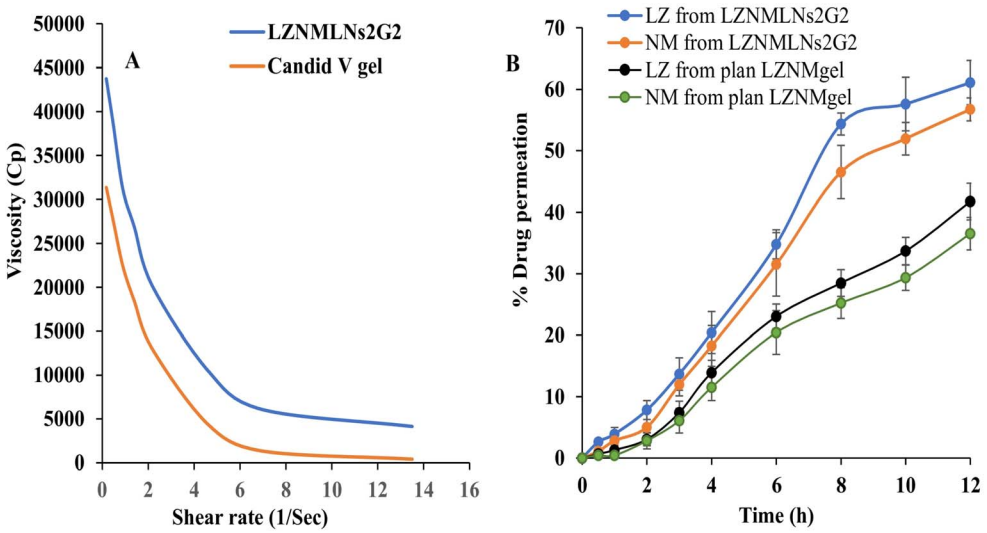

Fig. 4 (A) Rheological graph (flow curve) of (LZNMLNs2G3) and commercial (Candid V gel), showing the shear thinning system. (B) *Ex vivo* permeation of LZ and NM from LZNMLNs2G3 and LZNM gel.

Open Access Article. Published on 19 February 2025. Downloaded on 11/10/2025 1:52:29 AM.
This article is licensed under a Creative Commons Attribution-NonCommercial 3.0 Unported Licence.

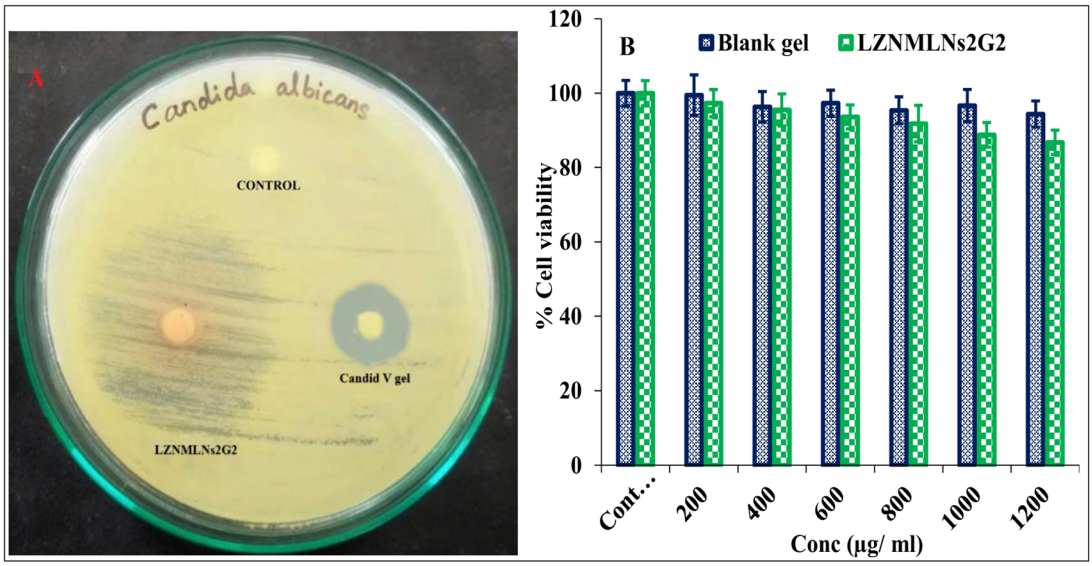

Fig. 5 (A) *In vitro* antimicrobial activity of experimental lipid nanocarrier-embedded bigel (LZNMLNs2G2) *via* agar well diffusion method against *Candida albicans vs.* standard gel (Candid V gel) as positive control. DMSO was used as negative control. (B) Cytotoxicity analysis of nano-bigel (LZNMLNs2G2)/blank gel in selected vaginal epithelial cells.

mL^{-1}, $0.097 \pm 0.25\ h^{-1}$, 7888.45 ± 92.71 ng h mL^{-1}, $54\,446.91 \pm 192.13$ ng h^2 mL^{-1}, $86\,823.81 \pm 198.02$ ng h^2 mL^{-1}, 7.13 ± 0.26 h and 7.84 ± 0.27 h, respectively. LZNMLNs2G2 exhibited significantly higher PK parameters than conventional LZNM gel. The $AUC_{0\text{-}t}$ of LZ and NM from the LZNMLNs2G2 were 1.94-fold and 1.33-fold higher than those of Candid V gel (commercial gel). LZNMLNs2G2 also exhibited a significantly higher MRT (1.49-fold for LZ and 1.39-fold for NM) compared to Candid V gel. This indicated sustained release of LZ and NM from LZNMLNs2G2, maintaining the therapeutic concentration over an extended period. The significantly lower elimination rate of LZ and NM from LZNMLNs2G2 compared to Candid V ($0.157 \pm 0.032\ h^{-1}$) further revealed the prolonged *in vivo* residence time of drugs from LZNMLNs2G2, which would be beneficial in enhancing the effectiveness of the treatment.

In vivo efficacy evaluation in vaginal candidiasis model

The *in vivo* efficacy of LZNMLNs2G2 compared to Candid V gel and blank gel was examined in female rabbits after the induction of vaginitis. The results are depicted in Fig. 6B.

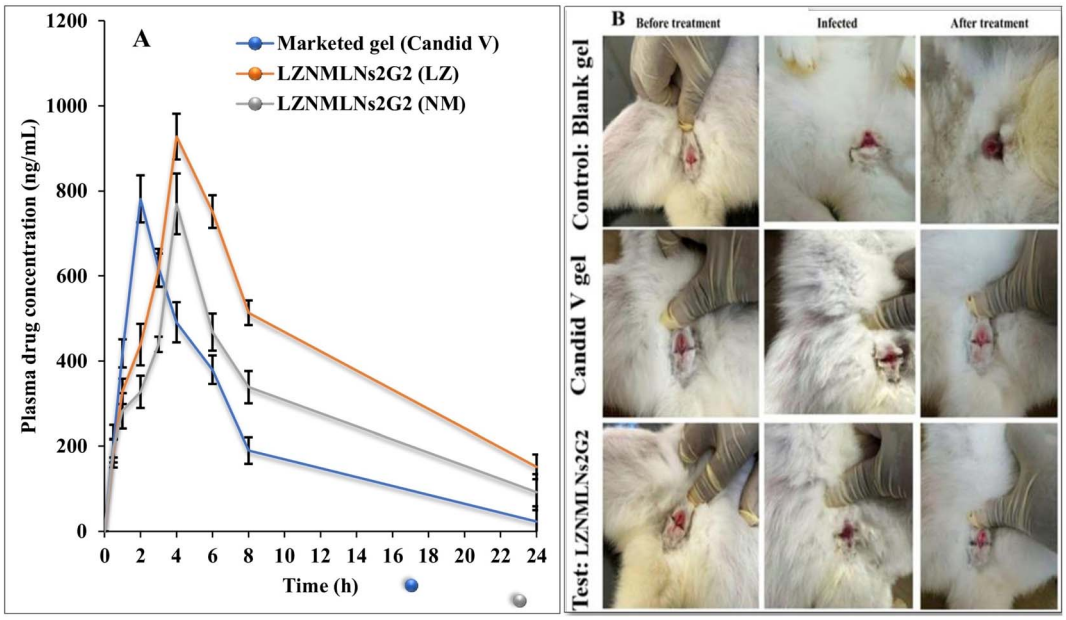

Fig. 6 (A) Plasma concentration of LZ and NM following topical vaginal application of experimental nanogel (LZNMLNs2G2) against commercial gel (Candid V gel). Data show mean ± SD ($n = 3$). (B) *In vivo* efficacy evaluation of experimental nanogel (LZNMLNs2G2) in vaginitis-induced rabbit model against commercial gel (Candid V gel).

 © 2025 The Author(s). Published by the Royal Society of Chemistry

Open Access Article. Published on 19 February 2025. Downloaded on 11/10/2025 1:52:29 AM.
This article is licensed under a Creative Commons Attribution-NonCommercial 3.0 Unported Licence.

Table 4 Estimation of plasma pharmacokinetic parameters in albino rabbits following topical vaginal application of Candid V gel (standard) and selected nano-biogels[a]

Parameters	Marketed gel (candid V)	LZNMLNs2G2 (LZ)	LZNMLNs2G2 (NM)
T_{max} (h)	2	4	4
C_{max} (ng mL^{-1})	781.13 ± 55.07	927.63 ± 38.667	769.21 ± 43.67
$AUC_{0\text{-}t}$ (ng h mL^{-1})	5199.60 ± 56.18	10 110.88 ± 143.87	6944.10 ± 78.93
K_{el} (h^{-1})	0.157 ± 0.032	0.087 ± 0.021	0.097 ± 0.25
$AUC_{0\text{-}inf}$ (ng h mL^{-1})	5346.78 ± 76.23	11 828.00 ± 103.87	7888.45 ± 92.71
$AUMC_{0\text{-}t}$ (ng h^2 mL^{-1})	29 349.84 ± 1121.32	83 542.28 ± 172.18	54 446.91 ± 192.13
$AUMC_{0\text{-}inf}$ (ng h^2 mL^{-1})	33 819.15 ± 172.19	144 276.01 ± 202.12	86 823.81 ± 198.02
Half-life (h)	4.41 ± 0.13	7.88 ± 0.21	7.13 ± 0.26
MRT (h)	5.64 ± 0.16	8.26 ± 0.24	7.84 ± 0.27

[a] Abbreviations: C_{max}: maximum plasma drug concentration; T_{max}: time taken in hours to attain maximum plasma drug concentration; AUC: area under the plasma concentration time curve; AUMC: area under the first moment curve; K_{el}: elimination rate constant; MRT: mean residence time.

LZNMLNs2G2 exhibited a considerable decrease (to <0.05) in an infection on the 7th day of treatment as compared to the Candid V gel on the 10th day. However, the blank gel group (Group III) did not show any significant improvement in infection. Following topical application across the infected area, LZNMLNs2G2-treated rabbits showed complete recovery within 7 days of treatment.

Docking analysis

Promising *in vitro/in vivo* antimicrobial results prompted us to investigate the affinities of LZ and NM for key proteins linked to *Candida albicans*. For LZ, higher binding affinity was observed for all the selected *Candida* proteins, among which docking with 14-α-demethylase (5TZ1) resulted in the highest docking score of −13.44 kcal mol^{-1} (Table 5). Similarly, binding affinities of −9.46 kcal mol^{-1}, −11.50 kcal mol^{-1} and −10.99 kcal mol^{-1} were observed for Als3 adhesin (4LE8), Crystal Structure of Enolase1 (7v67), and thymidylate synthase (5UIV) with LZ. Further, a higher binding affinity (−7.17 kcal-mol^{-1}) was observed for NM against 5UIV. The overall docking study rationalized the *in vitro* and *in vivo* antimicrobial test results.

Discussion

The goal of the current study was to improve the transepithelial delivery of LZ and NM through LN gel. Different batches of LZNMLNs with varying ratios of lipids (CHL and SL) at fixed concentrations of the drugs were prepared using the thin-film hydration method. The optimized LZNMLN (LZNMLNs2) formulation was selected based on Z-avg, drug loading %, and EE. The optimized formulation exhibited PDI < 0.5 (0.378), indicating the monodispersed or narrow size distribution of the vesicles. PDI > 0.5 indicates the broad size distribution of the vesicles of particles.[49]

The FESEM image showed the spherical shape and smooth morphology of LZNMLNs2 (Fig. 1C). The spherical size of the LNs would help to increase contact and adhesion with the vaginal wall. The smooth surface of the LNs may decrease irritation and enhance comfort during application.[50] In addition, spherically shaped particles increase drug permeation through the vaginal epithelium and improve drug absorption. They also allow the sustained release of encapsulated drugs over an extended period.[51]

The FESEM result was further supported by Cryo-TEM analysis. Cryo-TEM is an irreplaceable tool for the clear visualization of internal morphology and lamellarity. In the cryo-TEM of LZNMLNs2, clear unilamellar vesicles, without any structural damage were observed (Fig. 1D). The cryo-TEM image indicated that vesicle lamellarity did not significantly alter the suspension state in terms of size, shape or architecture.[52]

The FTIR spectra showed the absence of any major physical/chemical interaction between LZ/NM and other lipids/excipients used in formulating the LNs. However, a few minor shifts in characteristic peaks of drugs and lipids in the LZNMLNs were detected, which could be attributed to the presence of van der Waals, electrostatic, or dipole–dipole interactions between the components during the formulation process. Such minor physical interactions would be rather beneficial in holding the drugs together in the LNs (Fig. 2A). Similar types of observation have been reported for curcumin- and tetrandrine-loaded LNs.[53]

A DSC study was performed to analyze the crystallinity of the therapeutic agents in the LNs.[54] The sharp single endothermic peaks of pure LZ and NM indicated their purity and crystallinity (Fig. 2B). However, the absence of sharp endothermic peaks of LZ and NM in LZNMLNs2 indicated encapsulation of drugs inside the LNs with loss of their crystallinity or a change into an amorphous form, which would be helpful for improving their solubility.[55]

Similarly, the diffractograms of pure LZ and NM showed sharp, intense peaks indicating their crystalline nature, as supported by various reports.[56,57] However, in the diffractogram of LZNMLNs2, LZ and NM did not show sharp intense peaks (but diminished peaks) (Fig. 2C). This revealed that LZ and NM might lose crystallinity or change into an amorphous form. Induction of amorphization would be helpful for improving the solubility, bioavailability, and therapeutic activity of the drug.[56] In addition, the low intensity or absence of LZ and NM peaks in the LNs indicated the suitable encapsulation of the drugs into

Open Access Article. Published on 19 February 2025. Downloaded on 11/10/2025 1:52:29 AM.
This article is licensed under a Creative Commons Attribution-NonCommercial 3.0 Unported Licence.

Table 5 *In silico* docking analysis of selected *Candida albicans* proteins with luliconazole and niacinamide

RECEPTOR (PDB ID)	14- α-demethylase (5TZ1)	Sequanlene epoxidase (4MAI)	Delta(14)-sterol reductase (4QUV)	Thymidylate synthase (5UIV)
	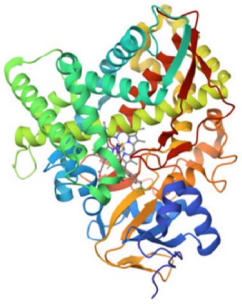		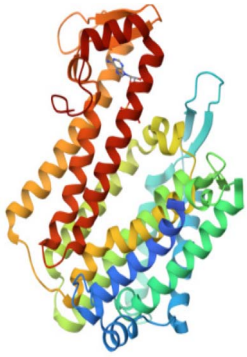	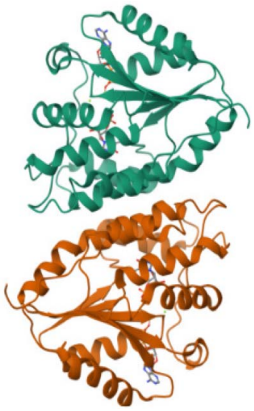
Luliconazole	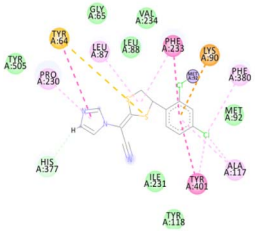 −13.4464	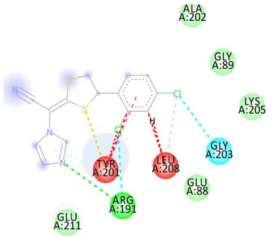 −8.8225	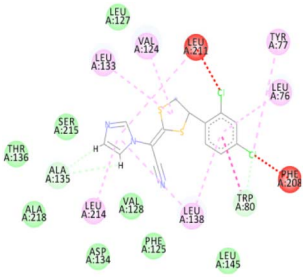 −12.235	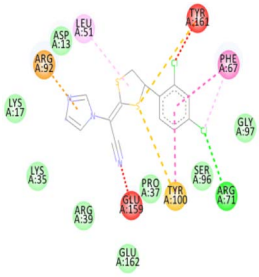 −10.9905
Niacinamide	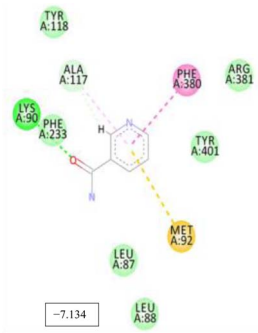 −7.134	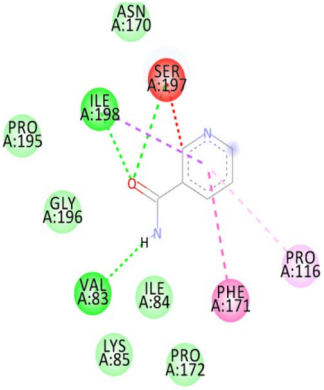 −8.4563	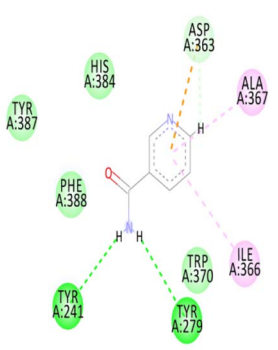 −7.9364	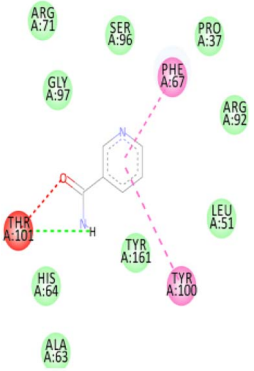 −7.1798

the LN matrix, which would be helpful in protecting the drugs from degradation and providing a sustained release profile.[58,59]

The *in vitro* release of LZ and NM from LZNMLNs2 was studied in simulated vaginal fluid (PBS, pH 4.2) using a dialysis bag. LZ and NM exhibited sustained release over the 24 h of the study (Fig. 3A). Owing to the hydrophilic nature of NM, it might be encapsulated deep inside the aqueous core of the LNs, which might result in slower release than for LZ. This result was confirmed by a previously published report of a tetracaine-hydrochloride-loaded lipid vesicle.[60] The sustained release of drugs from the LNs would maintain the therapeutic concentration over an extended period and would increase absorption as well as decrease side effects. It would also help to increase patient compliance by decreasing the dose and dosing frequency and related adverse effects.

Furthermore, among the kinetic models, the Higuchi kinetics model was found to be the best fit because it showed the highest R^2 value and followed the non-Fickian diffusion

 © 2025 The Author(s). Published by the Royal Society of Chemistry

Open Access Article. Published on 19 February 2025. Downloaded on 11/10/2025 1:52:29 AM. This article is licensed under a Creative Commons Attribution-NonCommercial 3.0 Unported Licence.

mechanism (erosion- and diffusion-controlled release) for the drug release pattern.[61]

LZNMLNs2-gels were successfully prepared using Carbopol-934P, HPMC-E15M, and *Azadirachta indica* gum. *Azadirachta indica* gum (a natural adhesive polymer) was used as a bio-adhesive agent to increase retention at the vaginal site. Additionally, *Azadirachta indica* gum possesses suitable antimicrobial properties, which would further synergize the antifungal potency. LZNMLNs2G2 (0.5% w/v neem gum, 0.8% w/v Carbopol-934P, and 1.5% w/v HPMC-E15M) was chosen as the optimized gel because it exhibited optimum gel characteristics (Table 2). Because of its excellent bio-adhesion, viscosity, and optimum swelling (Fig. 3B), LZNMLNs2G2 would remain for a long time on the application site, leading to an increase in permeation and therapeutic efficacy.[62]

LZNMLNs2G2 exhibited a shear-thinning system (Fig. 4A), *i.e.*, the viscosity of the gel decreased with increasing shear rate. This indicates that the gel followed pseudo-plastic flow (non-Newtonian flow).[63] This system may be easily spread over the application area and evenly distributed as well as controlling drug release. This system would be beneficial for effective *in vivo* application across the vaginal area.

An *ex vivo* permeation study of LZ and NM from LZNMLNs2G2 was performed, and the results are shown in Fig. 4B. LZNMLNs2G2 showed a significantly higher permeation of LZ and NM in 12 h than plain LZNM gel. The nanosize of LZNMLNs2, which provides a high surface area to the diffusion medium, led to high permeation of LZ and NM compared to plain LZNM gel. In addition, the higher permeation of drugs from LZNMLNs2G2 could be attributed to the high adhesion potential of the nanogel, which provided sufficient time for the drugs to come out of the gel matrix and permeate across the vaginal epithelium.[64] This finding agreed with a previously published report of clotrimazole-loaded LN gel for vaginal delivery.[65]

The antifungal activity of LZNMLNs2G2 against *Candida albicans* was determined using the agar well diffusion method. LZNMLNs2G2 exhibited significantly ($P < 0.05$) higher activity (ZOI: 34 ± 2 mm) than the commercial gel (Candid V gel, 2%, ZOI: 18 ± 1 mm) (Fig. 5A). The high antifungal activity of LZNMLNs2G2 might be due to the nanosize of the drug-loaded LNs, which provide a high surface area and might increase permeation of the fungal cell membrane, leading to enhanced activity. Moreover, the sustained release of medicaments from LZNMLNs2G2 over an extended period might be responsible for achieving higher antifungal activity than Candid V gel. A similar type of observation was reported in fluconazole-loaded LN gel, where a significantly higher ZOI (34 mm) was shown by LN gel than by plain gel (20 mm).[66]

A cytotoxicity study of LZNMLNs2G2 was undertaken to determine any potential toxicity to vaginal epithelial cells upon topical application. LZNMLNs2G2 and blank gel did not show any toxicity to vaginal epithelial cells, as evidenced by an MTT assay (Fig. 5B). Even at the highest concentration of drugs, no significant toxic effect on cells was observed (86.75 ± 3.29% cell viability at 1200 μg mL^{-1}). This revealed the non-toxic nature of LZNMLNs2G2 and its suitability for *in vivo* application for vaginal infections.

The PK parameters of LZ and NM for LZNMLNs2G2 after application into rabbits were analyzed and compared to Candid V gel, as depicted in Table 4 and Fig. 6A. LZNMLNs2G2 showed a significantly higher C_{max} AUC, AUMC, MRT, and half-life ($t_{1/2}$) of LZ and NM compared to Candid V gel. The MRT and low elimination rate of LZNMLNs2G2 revealed the good *in vivo* stability of the drugs. Additionally, it may be attributed to the nanosize of the particles, the higher stability of the encapsulated drugs, the bio-adhesive characteristic of the gel and the sustained released of drugs into the vaginal microenvironment. It can be revealed that the nanogel could be a good carrier for the topical treatment of vaginal infection.

LZNMLNs2G2 showed significantly better *in vivo* activity than the commercial gel (Candid V gel) in the disease-induced rabbit model. Infection-induced rabbits exhibited complete recovery from vaginal infection after 7 days of treatment with LZNMLNs2G2 (Fig. 6B). LZNMLNs2G2 exhibited high activity owing to an increase in solubility, protection of the drugs from untimely degradation, and an increase in the vaginal epithelial permeation, which led to an increase in bioavailability and therapeutic efficacy.

Docking data revealed higher docking scores for both LZ and NM against all selected *Candida* proteins. However, the docking score of LZ was considerably higher than that of NM. Appropriate molecular interaction between the drugs and selected fungal protein further rationalized our approach for the co-delivery of both drugs in LN carriers.

Conclusion

The present research developed an LZNM-loaded LN gel as a novel topical delivery method to improve therapeutic efficacy against vaginal candidiasis. LZNMLNs2 was found to be nano-sized and spherical, with a high loading of LZ and NM. LZNMLNs2G2 showed excellent viscosity, spreadability, bio-adhesion, and swelling index, as well as significantly higher *ex vivo* vaginal epithelial permeation. Impressive *in vitro* antifungal activity of LZNMLNs2G2 was observed against *Candida albicans* cells. An MTT assay showed the nontoxic and biocompatible nature of the LZNMLNs2G2 formulation. *In vivo* studies showed higher therapeutic effectiveness of LZNMLNs2G2 than commercial gel (Candid V gel) in vaginitis-induced rabbits. Based on the *in vitro*, *in vivo*, and *in silico* results, LZNMLNs2G2 may be considered a suitable option for the treatment of vaginal candidiasis. The outcome of this study will lay the foundations for further research on comparative efficacy analysis of LZNMLNs2G2 in other *in vivo* vaginitis models, toxicity studies, and *in vitro*/*in vivo* correlation analysis toward its future clinical translation.

Ethical statement

The study complied with the ARRIVE guidelines, and was carried out in accordance with the U.K. Animals (Scientific

Open Access Article. Published on 19 February 2025. Downloaded on 11/10/2025 1:52:29 AM.
This article is licensed under a Creative Commons Attribution-NonCommercial 3.0 Unported Licence.

Procedures) Act, 1986 and associated guidelines, EU Directive 2010/63/EU for animal experiments.

Data availability

All the data for the manuscript is available in the manuscript.

Author contributions

Bhabani Sankar Satapathy: methodology, conceptualization, investigation, software, resources, writing – original draft, Ameeduzzafar Zafar: software, writing – original draft, writing – review & editing; Musarrat Husain Warsi: data curation, writing – review & editing Sritam Behera: investigation, resources; Dibya lochan Mohanty: methodology, resources; Md Ali Mujtaba: writing – review & editing, visualization. Mahaprasad Mohanty: methodology, writing – review & editing. Atul Kumar Upadhyay: data curation, writing – review & editing. Mohammad Khalid: writing – review & editing, data curation.

Conflicts of interest

No conflict of interest

Acknowledgements

The authors extend their appreciation to Taif University, Saudi Arabia, for supporting this work through project number (TU-DSPP-2024-136).

References

1 A. Aklilu, M. Woldemariam, A. Manilal, G. Koira, R. M. Alahmadi, G. Raman, A. Idhayadhulla and M. Yihune, Aerobic vaginitis, bacterial vaginosis, and vaginal candidiasis among women of reproductive age in Arba Minch, southern Ethiopia, *Sci. Rep.*, 2024, **14**(1), 9813.

2 A. Ahuja and M. Bajpai, Nanoformulations Insights: A Novel Paradigm for Antifungal Therapies and Future Perspectives, *Curr. Drug Delivery*, 2024, **21**(9), 1241–1272.

3 C. de, J. Orlandi Sardi, D. R. Silva, P. C. Anibal, J. J. de Campos Baldin, S. R. Ramalho, P. L. Rosalen, M. L. Macedo and J. F. Hofling, Vulvovaginal candidiasis: epidemiology and risk factors, pathogenesis, resistance, and new therapeutic options, *Curr. Fungal Infect. Rep.*, 2021, **15**, 32–40.

4 C. Chayachinda, M. Thamkhantho, T. Rekhawasin and C. Klerdklinhom, Sertaconazole 300 mg *versus* clotrimazole 500 mg vaginal suppository for treating pregnant women with acute vaginal candidiasis: a double-blinded, randomized trial, *BMC Pregnancy Childbirth*, 2024, **24**(1), 1–8.

5 P. Kumar, D. K. Sharma and M. S. Ashawat, Topical creams of piperine loaded lipid nanocarriers for management of atopic dermatitis: development, characterization, and *in vivo* investigation using BALB/c mice model, *J. Liposome Res.*, 2022, **32**(1), 62–73.

6 Z. Vanić, M. W. Jøraholmen and N. Škalko-Basnet, Nanomedicines for the topical treatment of vulvovaginal infections: Addressing the challenges of antimicrobial resistance, *Adv. Drug Delivery Rev.*, 2021, **178**, 113855.

7 V. De Leo, F. Milano, A. Agostiano and L. Catucci, Recent advancements in polymer/liposome assembly for drug delivery: From surface modifications to hybrid vesicles, *Polymers*, 2021, **13**(7), 1027.

8 K. Ghosal, A. Pani, T. Chowdhury, A. Kundu and S. Thomas, Multi-vesicular Liposome and its Applications: A Novel Chemically Modified Approach for Drug Delivery Application, *Mini-Rev. Med. Chem.*, 2024, **24**(1), 26–38.

9 N. M. Badawi, M. A. Elkafrawy, R. M. Yehia and D. A. Attia, Clinical comparative study of optimized metronidazole loaded lipid nanocarrier vaginal emulgel for management of bacterial vaginosis and its recurrence, *Drug Delivery*, 2021, **28**(1), 814–825.

10 B. Mukherjee, S. Das, S. Chakraborty, B. Sankar Satapathy, P. Jyoti Das, L. Mondal, C. Mobaswar Hossain, N. Shekhar Dey and A. Chaudhury, Potentials of polymeric nanoparticle as drug carrier for cancer therapy: with a special reference to pharmacokinetic parameters, *Curr. Drug Metab.*, 2014, **15**(6), 565–580.

11 C. M. Caramella, S. Rossi, F. Ferrari, M. C. Bonferoni and G. Sandri, Mucoadhesive and thermogelling systems for vaginal drug delivery, *Adv. Drug Delivery Rev.*, 2015, **92**, 39–52.

12 H. Labie and M. Blanzat, Hydrogels for dermal and transdermal drug delivery, *Biomater. Sci.*, 2023, **11**(12), 4073–4093.

13 S. A. Mustfa, E. Maurizi, J. McGrath and C. Chiappini, Nanomedicine approaches to negotiate local biobarriers for topical drug delivery, *Adv. Ther.*, 2021, **4**(1), 2000160.

14 L. Song, F. Cao, S. Niu, M. Xu, R. Liang, K. Ding, Z. Lin, X. Yao and D. Liu, Population Pharmacokinetic/Pharmacodynamic Analysis of the Glucokinase Activator PB201 in Healthy Volunteers and Patients with Type 2 Diabetes Mellitus: Facilitating the Clinical Development of PB201 in China, *Clin. Pharmacokinet.*, 2024, **63**(1), 93–108.

15 L. Zhang, D. Pornpattananangku, C. M. Hu and C. M. Huang, Development of nanoparticles for antimicrobial drug delivery, *Curr. Med. Chem.*, 2010, **17**(6), 585–594.

16 M. Rani, K. Parekh, T. Mehta and A. Omri, Formulation development and characterization of luliconazole loaded—mesoporous silica nanoparticles (MCM— 48) as topical hydrogel for the treatment of cutaneous candidiasis, *J. Drug Delivery Sci. Technol.*, 2024, **91**, 105250.

17 Y. C. Boo, Mechanistic basis and clinical evidence for the applications of nicotinamide (niacinamide) to control skin aging and pigmentation, *Antioxidants*, 2021, **10**(8), 1315.

18 Z. Zhen, X. Xiong, Y. Liu, J. Zhang, S. Wang, L. Li and M. Gao, NaCl inhibits citrinin and stimulates Monascus pigments and monacolin K production, *Toxins*, 2019, **11**(2), 118.

19 S. A. Esfahani, M. Khoshneviszadeh, M. R. Namazi, A. Noorafshan, B. Geramizadeh, E. Nadimi and S. T. Razavipour, Topical nicotinamide improves tissue

 © 2025 The Author(s). Published by the Royal Society of Chemistry

Open Access Article. Published on 19 February 2025. Downloaded on 11/10/2025 1:52:29 AM.
This article is licensed under a Creative Commons Attribution-NonCommercial 3.0 Unported Licence.

regeneration in excisional full-thickness skin wounds: A stereological and pathological study, *Trauma Mon.*, 2015, **20**(4), e18193.

20 C. Marques, F. Hadjab, A. Porcello, K. Lourenço, C. Scaletta, P. Abdel-Sayed, N. Hirt-Burri, L. A. Applegate and A. Laurent, Mechanistic insights into the multiple functions of niacinamide: Therapeutic implications and cosmeceutical applications in functional skincare products, *Antioxidants*, 2024, **13**(4), 425.

21 M. Sanati and S. A. Yavari, Liposome-integrated hydrogel hybrids: Promising platforms for cancer therapy and tissue regeneration, *J. Controlled Release*, 2024, **368**, 703–727.

22 B. S. Satapathy, L. A. Kumar, G. Pattnaik and B. Barik, Lomustine Incorporated Lipid Nanostructures Demonstrated Preferential Anticancer Properties in C6 Glioma Cell Lines with Enhanced Pharmacokinetic Profile in Mice, *Acta Chim. Slov.*, 2021, **68**(4), 970–982.

23 B. S. Satapathy, P. K. Sahoo, S. Pattnaik, A. K. Nayak, L. Maharana and R. N. Sahoo, Conveyance of sofosbuvir through vesicular lipid nanocarriers as an effective strategy for management of viral meningitis, *RSC Adv.*, 2023, **13**(47), 33500–33513.

24 L. Tu, J. Zeng, X. Bai, Z. Wu, J. Wu and S. Xu, Nanoliposome-Mediated Encapsulation of Chlorella Oil for the Development of a Controlled-Release Lipid-Lowering Formulation, *Foods*, 2024, **13**(1), 158.

25 C. Singh, K. Rao, N. Yadav, N. Bansal, Y. Vashist, S. Kumari and P. Chugh, A Review: Drug Excipient Incompatibility by Ftir Spectroscopy, *Curr. Pharm. Anal.*, 2023, **19**(5), 371–378.

26 W. Li, M. Chountoulesi, L. Antoniadi, A. Angelis, J. Lei, M. Halabalaki, C. Demetzos, S. Mitakou, L. A. Skaltsounis and C. Wang, Development and physicochemical characterization of nanoliposomes with incorporated oleocanthal, oleacein, oleuropein and hydroxytyrosol, *Food Chem.*, 2022, **384**, 132470.

27 H. Bakeshlou, S. Pirsa, F. Mohtarami and M. Bener, Investigating the Structural and Antimicrobial Properties of Wheat Gluten Nanocomposite Film Containing Zinc Oxide Nanoparticles and Quercetin Nanoliposomes, *J. Environ. Polym. Degrad.*, 2024, 1–20.

28 M. Lei, G. Ma, S. Sha, X. Wang, H. Feng, Y. Zhu and X. Du, Dual-functionalized liposome by co-delivery of paclitaxel with sorafenib for synergistic antitumor efficacy and reversion of multidrug resistance, *Drug Delivery*, 2019, **26**(1), 262–272.

29 X. Zhang, Z. Wu, W. Zhang, L. Wang, P. Zhao, X. Lv, P. Guo and J. Chen, Surface modification by chitosan for improving stability and antioxidative activity of astaxanthin-loaded liposomes, *LWT–Food Sci. Technol.*, 2024, **198**, 116033.

30 S. Gholizadeh, H. Almasi, S. Amjadi, M. Moradi, N. Ghadiri Alamdari, S. Salmasi and E. Divsalar, Development and characterization of active packaging system based on zein nanofibers mat incorporated with geraniol-loaded nanoliposomes, *Food Sci. Nutr.*, 2024, **12**, 5373–5387.

31 T. Li, C. J. Nowell, D. Cipolla, T. Rades and B. J. Boyd, Direct comparison of standard transmission electron microscopy and cryogenic-TEM in imaging nanocrystals inside liposomes, *Mol. Pharm.*, 2019, **16**(4), 1775–1781.

32 B. Wang, X. C. Yu, S. F. Xu and M. Xu, Paclitaxel and etoposide co-loaded polymeric nanoparticles for the effective combination therapy against human osteosarcoma, *J. Nanobiotechnol.*, 2015, **13**, 1.

33 B. Pyrak, K. Rogacka-Pyrak, T. Gubica and Ł. Szeleszczuk, Exploring cyclodextrin-based nanosponges as drug delivery systems: Understanding the physicochemical factors influencing drug loading and release kinetics. nt, *J. Mol. Sci.*, 2024, **25**(6), 3527.

34 D. Sudipta, P. K. Haldar and G. Pramanik, Formulation and evaluation of herbal gel containing *Clerodendrum infortunatum* leaves extract, *Int. J. PharmTech Res.*, 2011, **3**, 140–143.

35 Y. Kimura, S. Shimizu and K. Haraguchi, Gelation and anomalous viscosity dynamics in aqueous dispersions of synthetic hectorite, *NPG Asia Mater.*, 2022, **14**(1), 27.

36 G. Sharma, M. K. Saini, K. Thakur, N. Kapil, N. K. Garg, K. Raza, V. G. Goni, A. Pareek and O. P. Katare, Aceclofenac cocrystal nanoliposomes for rheumatoid arthritis with better dermatokinetic attributes: a preclinical study, *Nanomed*, 2017, **12**(6), 615–638.

37 I. L. Dejeu, L. G. Vica□, L. L. Vlaia, T. Jurca, M. E. Mure□an, A. Pallag, G. H. Coneac, I. V. Olariu, A. M. Mu□, A. S. Bodea and G. E. Dejeu, Study for evaluation of hydrogels after the incorporation of liposomes embedded with caffeic acid, *Pharmaceuticals*, 2022, **15**(2), 175.

38 A. Mousavi Moghadam, M. Vafaie Sefti, M. Baghban Salehi and A. Dadvand Koohi, Preformed particle gel: evaluation and optimization of salinity and pH on equilibrium swelling ratio, *J. Pet. Explor. Prod. Technol.*, 2012, **2**, 85–91.

39 A. Ortega, A. B. da Silva, L. M. da Costa, K. C. Zatta, G. R. Onzi, F. N. da Fonseca, S. S. Guterres and K. Paese, Thermosensitive and mucoadhesive hydrogel containing curcumin-loaded lipid-core nanocapsules coated with chitosan for the treatment of oral squamous cell carcinoma, *Drug Delivery Transl. Res.*, 2023, **13**(2), 642–657.

40 S. Salah, G. E. Awad and A. I. Makhlouf, Improved vaginal retention and enhanced antifungal activity of miconazole microsponges gel: Formulation development and *in vivo* therapeutic efficacy in rats, *Eur. J. Pharm. Sci.*, 2018, **114**, 255–266.

41 S. Austermeier, M. Pekmezović, P. Porschitz, S. Lee, N. Kichik, D. L. Moyes, J. Ho, N. K. Kotowicz, J. R. Naglik, B. Hube and M. S. Gresnigt, Albumin neutralizes hydrophobic toxins and modulates Candida albicans pathogenicity, *mBio*, 2021, **12**(3), 10–128.

42 S. Mukherjee; P. Malik and T. K. Mukherjee, in Experimental Mammalian Cell Culture-Based Assays, ed. Mukherjee, T. K., Malik, P. and Mukhopadhyay, S., *Practical Approach to Mammalian Cell and Organ Culture*. Springer, Singapore, 2023, doi: DOI: 10.1007/978-981-19-1731-8_16-1.

43 A. Rajput, G. Shevalkar, K. Pardeshi and P. Pingale, Computational Nanoscience and Technology, *OpenNano*, 2023, **12**, 100147.

Open Access Article. Published on 19 February 2025. Downloaded on 11/10/2025 1:52:29 AM.
This article is licensed under a Creative Commons Attribution-NonCommercial 3.0 Unported Licence.

44 X. Zhao, D. Sun, A. Zhang, H. Huang, Y. Li and D. Xu, Candida albicans-induced activation of the TGF-β/Smad pathway and upregulation of IL-6 may contribute to intrauterine adhesion, *Sci. Rep.*, 2023, **13**(1), 579.

45 K. Atz, L. Cotos, C. Isert, M. Håkansson, D. Focht, M. Hilleke, D. F. Nippa, M. Iff, J. Ledergerber, C. C. Schiebroek and V. Romeo, Prospective *de novo* drug design with deep interactome learning, *Nat. Commun.*, 2024, **15**(1), 3408.

46 P. R. Murumkar, M. K. Sharma, P. Gupta, N. M. Patel and M. R. Yadav, Selection of suitable protein structure from protein data bank: an important step in structure-based drug design studies, *Mini-Rev. Med. Chem.*, 2023, **23**(3), 246–264.

47 C. Sharma, S. Gulati, N. Thakur, B. P. Singh, S. Gupta, S. Kaur, S. K. Mishra, A. K. Puniya, J. P. S. Gill and H. Panwar, Antibiotic sensitivity pattern of indigenous lactobacilli isolated from curd and human milk samples, *3 Biotech.*, 2017, **7**(1), 53.

48 J. W. Song, Y. S. Liu, Y. R. Guo, W. X. Zhong, Y. P. Guo and L. Guo, Nano-Liposomes Double Loaded with Curcumin and Tetrandrine: Preparation, Characterization, Hepatotoxicity and Anti-Tumor Effects, *Int. J. Mol. Sci.*, 2022, **23**(12), 6858.

49 B. Hoseini, M. R. Jaafari, A. Golabpour, A. A. Momtazi-Borojeni, M. Karimi and S. Eslami, Application of ensemble machine learning approach to assess the factors affecting size and polydispersity index of liposomal nanoparticles, *Sci. Rep.*, 2023, **13**(1), 18012.

50 H. Nsairat, D. Khater, U. Sayed, F. Odeh, A. Al Bawab and W. Alshaer, Liposomes: structure, composition, types, and clinical applications, *Heliyon*, 2022, **8**(5), e09394.

51 J. Kuntsche, J. C. Horst and H. Bunjes, Cryogenic transmission electron microscopy (cryo-TEM) for studying the morphology of colloidal drug delivery systems, *Int. J. Pharm.*, 2011, **417**(1–2), 120–137.

52 S. Handali, E. Moghimipour, M. Kouchak, Z. Ramezani, M. Amini and K. A. Angali, New folate receptor targeted nano liposomes for delivery of 5-fluorouracil to cancer cells: strong implication for enhanced potency and safety, *Life Sci.*, 2019, **227**, 39–50.

53 B. Zhai, Q. Wu, W. Wang, M. Zhang, X. Han, Q. Li, P. Chen, X. Chen, X. Huang, G. Li, Q. Zhang, R. Zhang, Y. Xiang, S. Liu, T. Duan, J. Lou, T. Xie and X. Sui, Preparation, characterization, pharmacokinetics and anticancer effects of PEGylated β-elemene liposomes, *Cancer Biol. Med.*, 2020, **17**(1), 60–75.

54 A. Khare, I. Singh, P. Pawar and K. Grover, Design and Evaluation of Voriconazole Loaded Solid Lipid Nanoparticles for Ophthalmic Application, *J. Drug Delivery*, 2016, **2016**, 6590361.

55 Z. Rahman, A. S. Zidan and M. A. Khan, Non-destructive Methods of Characterization of Risperidone Solid Lipid Nanoparticles, *Eur. J. Pharm. Biopharm.*, 2010, **76**, 127–137.

56 T. Fawcett, S. Kabekkodu, J. Blanton, C. Crowder and T. Blanton, Simulation Tools and References for the Analysis of Nanomaterials, *Adv. X-Ray Anal.*, 2015, **58**, 108–120.

57 S. Banerjee, S. Roy, K. Nath Bhaumik, P. Kshetrapal and J. Pillai, Comparative study of oral lipid nanoparticle formulations (LNFs) for chemical stabilization of antitubercular drugs: physicochemical and cellular evaluation, *Artif. Cells, Nanomed., Biotechnol.*, 2018, **46**(sup1), 540–558.

58 S. Pande, Liposomes for drug delivery: review of vesicular composition, factors affecting drug release and drug loading in liposomes, *Artif. Cells, Nanomed., Biotechnol.*, 2023, **51**(1), 428–440.

59 N. Akombaetwa, A. B. Ilangala, L. Thom, P. B. Memvanga, B. A. Witika and A. B. Buya, Current Advances in Lipid Nanosystems Intended for Topical and Transdermal Drug Delivery Applications, *Pharmaceutics*, 2023, **15**(2), 656.

60 Y. Jiang, F. Li, Y. Luan, W. Cao, X. Ji, L. Zhao, L. Zhang and Z. Li, Formation of drug/surfactant catanionic vesicles and their application in sustained drug release, *Int. J. Pharm.*, 2012, **436**(1–2), 806–814.

61 Y. Fu and W. J. Kao, Drug release kinetics and transport mechanisms of non-degradable and degradable polymeric delivery systems, *Expert Opin. Drug Delivery*, 2010, **7**(4), 429–444.

62 T. Osmałek, A. Froelich, B. Jadach, A. Tatarek, P. Gadziński, A. Falana, K. Gralińska, M. Ekert, V. Puri, J. Wrotyńska-Barczyńska and B. Michniak-Kohn, Recent Advances in Polymer-Based Vaginal Drug Delivery Systems, *Pharmaceutics*, 2021, **13**(6), 884.

63 T. Sanz Taberner, A. Martín-Villodre, J. M. Pla-Delfina and J. V. Herráez, Consistency of Carbopol 971-P NF gels and influence of soluble and cross-linked PVP, *Int. J. Pharm.*, 2002, **233**(1–2), 43–50.

64 C. K. Enggi, H. T. Isa, S. Sulistiawati, K. A. R. Ardika, S. Wijaya, R. M. Asri, S. A. Mardikasari, R. F. Donnelly and A. D. Permana, Development of thermosensitive and mucoadhesive gels of cabotegravir for enhanced permeation and retention profiles in vaginal tissue: A proof of concept study, *Int. J. Pharm.*, 2021, **609**, 121182.

65 M. Ning, Z. Gu, H. Pan, H. Yu and K. Xiao, Preparation and *in vitro* evaluation of liposomal/niosomal delivery systems for antifungal drug clotrimazole, *Indian J. Exp. Biol.*, 2005, **43**(2), 150–157.

66 R. Nanda, R. S. Narang and J. K. Narang, Design and Characterization of Fluconazole Loaded Elastic Liposome Based Gel for Treatment of Keratomycosis, *FABAD J. Pharm. Sci.*, 2022, **47**(2), 161–174.

 © 2025 The Author(s). Published by the Royal Society of Chemistry